SCHOOL OF COMPUTATION, INFORMATION AND TECHNOLOGY — PROFESSORSHIP FOR QUANTUM COMPUTING

TECHNISCHE UNIVERSITÄT MÜNCHEN

Bachelor's Thesis in Electrical Engineering and Information Technology

Variational Fitting of the Bath Correlation Function as a Sum of Exponential Functions

Author: Yigit Serbest
Supervisor: Richard Milbradt
Advisor: Prof. Dr. Christian B. Mendl
Submission Date: 31.03.2025

I confirm that this bachelor's thesis is my own work and I have documented all sources and material used.

Munich, 31.03.2025 Yigit Serbest

Acknowledgments

I would like to extend my thanks to my supervisor, Richard Milbradt, for his support throughout the thesis. Our discussions and his insights have proven themselves more than valuable and I appreciate his guidance.

I also would like to acknowledge the usage of digital tools for assistance. OpenAI's ChatGPT and Grammarly were utilized to clarify the concepts and arguments as well as improving the grammar and the readability of the thesis. These tools were utilized as supplementary aids.

Abstract

This thesis focuses on the decompositions of the bath correlation function using an Ohmic spectral density. The calculation of the bath correlation function yields high computational effort. Hence we used a definition consisting of a sum of exponential functions to define the bath correlation function in order to simplify the computation. The Gradient Descent Algorithm is used for the optimal approximation of the bath correlation function.

Contents

1 Introduction **6**

2 Background **7**
2.1 Open quantum systems 7
2.2 Spectral density 8

3 Theoretical Framework **9**
3.1 The Bath Correlation Function 9
3.2 Variational Fitting 10

4 Methodology **11**
4.1 Gradient Descent for Optimization 11
4.2 Numerical Implementation 12
4.2.1 Parameters 12
4.2.2 Approximation and Optimization 13
4.2.3 L2 Regularization 14
4.2.4 K Regularization 15

5 Results and Discussion **16**

6 Conclusion **21**

7 List of Figures **22**

8 Bibliography **23**

1 Introduction

Open quantum system are in constant interaction with their external environments. These systems are pivotal in understanding various occurring phenomena in physics and chemistry. The bath correlation function is fundamental in the characterization of the aforementioned interactions, providing insights into the dynamics of the system and decoherence processes.

The quantum interactions between the system of interest and the environment lead to energy exchange and entanglement. Decoherence is observed as a result, where the system's quantum behavior diminishes due to the influences of the external environment. It is essential to model these interactions accurately in order to predict the system behavior and design quantum technologies.

The influence of the environmental fluctuations over time is quantified by the bath correlation function. The bath correlation function entails information regarding the environment's spectral properties and its influence on the system. In that sense, it is crucial to be able to understand and properly evaluate this function in order to effectively model open quantum systems. In these open quantum system models the environment is often modeled as an infinite number of harmonic oscillators that couple linearly to some system degrees of freedom. It is convenient to describe the impact of the environment on the system using a spectral density, which contains information about the spectrum of the environment as well as the frequency-dependent coupling.[1, 2, 3, 4]

This thesis aims to investigate variational fitting techniques for approximating the bath correlation function as a sum of exponential functions. The bath correlation function in its integral form is relatively simple in terms of calculation. However,the traditional formulations of the bath correlation function and methods such as the Hierarchy of Pure States (HOPS) and the Hierarchical Equations of Motion (HEO) involve multiple integrations of the bath correlation function which yield high computational intensity and complexity. The approximation serves the simplification of complex interactions, making them more tractable for analytical and numerical analyses. Hence, reducing the computational complexity for the evaluation of the interactions.

2 Background

2.1 Open quantum systems

Various phenomena in physics do not comply to the laws of classical mechanics. Hence, open quantum systems are pivotal to model these phenomena and to predict their behaviors. These systems interact with their environments, which leads to energy exchange and entanglement.[6, 7, 8] If the environment's impact causes the system's quantum behavior to diminish, the system experiences decoherence [8].

The spin-boson model is fundamental for the description of how a two-state system (TSS) interacts with the surrounding bosonic environment (bath) [6]. This model is widely applied in quantum optics, condensed matter physics and quantum computing, where understanding decoherence and dissipation is crucial. The two-state system represents an open quantum system with two discrete energy states, similar to a quantum bit (qubit) in computing or an electron spin in a magnetic field. The subatomic particles called 'bosons' have an integer spin. The environment is a bosonic bath, which consists of and infinite number of harmonic oscillators (bosons) [7]. The bosons appear on distinct energy levels, hence it is possible for dissipation to occur when a boson is coupled to another particle. The TSS and the environment exchange energy, leading to dissipation and decoherence as shown in Figure1.

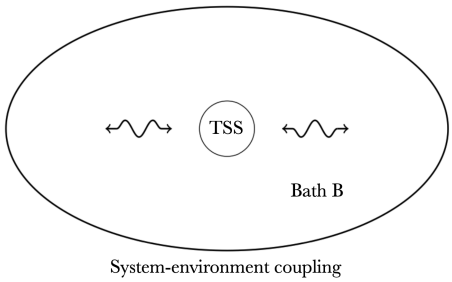

Figure 1: Schematics of the total system consisting of the two-state system TSS and the bath B

The quantum two-time bath correlation function quantifies the interactions between the bath and the two-state system, which often is a two-state particle. The generic Hamiltonian of a system coupled to a bath, in the absence of external fields, can be expressed as

$$\hat{H} = \hat{H}_(\mathbf{q,p}) + \hat{H}_B(\mathbf{Q,P}) + \hat{H}_{SB}(\mathbf{q,p,Q,P}), \tag{1}$$

where $\hat{H}_s$ is the system Hamiltonian, $\hat{H}_B$ is the bath Hamiltonian, $\hat{H}_{SB}$ is the system-bath Hamiltonian. In addition, $(\mathbf{q}, \mathbf{p}) = (q_j, p_j)$ and $(\mathbf{Q}, \mathbf{P}) = (Q_k, P_k)$, indicate the generalized multidimensional conjugated coordinates for the system and the bath, respectively [5].

2.2 Spectral density

The spectral density $J(\omega)$ describes the frequency dependent coupling of the system to the bath. The spectral density function is necessary to calculate the bath correlation function. Although there are different definitions for the spectral density function in the quantum literature, we will be using the spectral density with exponential cutoff.

$$J(\omega) = \eta\omega^s e^{-\frac{\omega}{\omega_c}}, \tag{2}$$

where ω_c is the cutoff frequency and η scales the overall strength [1][19][20]. The spectral density function $J(\omega) = \eta\omega^s e^{-\frac{\omega}{\omega_c}}$ encompasses various spectral densities depending on the value of the **Ohmic parameter s**:

- **Ohmic Spectral Density**: When $s = 1$, the spectral density is linear in ω, representing a direct proportionality. This form is typical in systems where the environment induces a friction-like effect on the system.
- **Sub-Ohmic Spectral Density**: For $s < 1$, the spectral density grows slower than linearly with ω, indicating weaker coupling at low frequencies. This scenario is relevant in systems where low-frequency environmental modes dominate the interaction.
- **Super-Ohmic Spectral Density**: When $s > 1$, the spectral density increases faster than linearly with ω, suggesting stronger coupling at higher frequencies. This situation arises in environments where high-frequency modes have a more significant impact on the system.

The parameter η denotes the coupling strength between the system and the environment, while ω_c is the cutoff frequency ensuring that $J(\omega)$ diminishes for large ω [12]. This behavior reflects the physical reality that environmental modes beyond a certain frequency have negligible influence on the system. For the purpose of this thesis, each of the parameters η, s and ω_c will hold a random value within an interval of their typical values. Therefore, the variational fitting process will not optimize by adapting to set parameters.

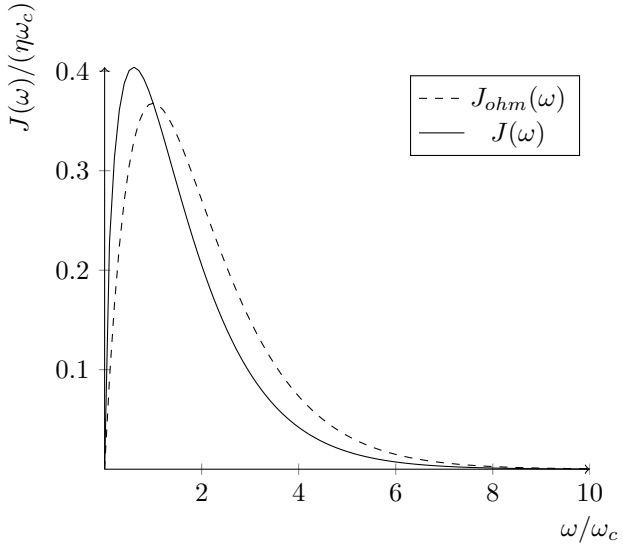

Figure 2: $J(\omega)/(\eta\omega_c)$ plotted in terms of ω/ω_c

3 Theoretical Framework

3.1 The Bath Correlation Function

The bath correlation function describes the influence of the environment on a system. The correlator $C(t)$ is in general complex and one can show, see,w.g., Refs. [14] and [15], that it has the following symmetries with respect to time [5]:

$$C(-t) = C^*(t) = C(t - i\beta\hbar). \tag{3}$$

In the research article "On the alternatives for bath correlators and spectral densities from mixed quantum-classical simulations" by Stéphanie Valleau, Alexander Eisfeld, and Alán Aspuru-Guzik have utilized the Fourier transform of the time correlation function to derive the definition of the bath correlation function[5]. First, the Fourier transform of the time correlation function is defined

$$G(\omega) \equiv \mathcal{F}[C(t)](\omega) = \int_{-\infty}^{\infty} e^{i\omega t} C(t) dt. \tag{4}$$

The function $G(\omega)$ is referred to as the temperature-dependent coupling density [5]. $C(t)$ has real and imaginary parts. Hence $G(\omega)$ can be split into a symmetric and antisymmetric component using the convention of Ref. [13].

$$G(\omega) = G_{sym}(\omega) + G_{asymm}(\omega), \tag{5}$$

$$G_{sym/asymm}(\omega) = \frac{1}{2}(G(\omega) \pm G(-\omega)). \tag{6}$$

The time symmetry in Eq.3 implies that $G(\omega)$ is related to its antisymmetric part by

$$G(\omega) = \frac{2}{1 - e^{-\beta\hbar\omega}} G_{asymm}(\omega) \tag{7}$$

$$= (1 + \coth(\beta\hbar\omega/2)) G_{asymm}(\omega) \tag{8}$$

It will be convenient to abbreviate $G_{asymm}(\omega)$ by defining

$$J(\omega) \equiv G_{asymm}(\omega).$$

[5] Using both the definition of $G(\omega)$, Eq.4, and the relation in Eq.7, the correlation function can be defined as:

$$C(t) = \frac{1}{2\pi} \int_{-\infty}^{\infty} J(\omega) \left[coth\left(\frac{\beta\hbar\omega}{2}\right) + 1 \right] e^{-i\omega t} d\omega \tag{9}$$

This function as itself yields high computational effort and less than optimal runtime with regards to HOPS and HEO methods.

3.2 Variational Fitting

The coth function as an integrand results in poor performance while computing. Therefore instead of numerically integrating the full function, we approximate it using a sum of exponential functions:

$$C_{approx}(t) = \sum_{j=1}^{K} g_j e^{-i\omega_j t} \tag{10}$$

The coefficients g_j and frequencies ω_j are to be optimized using gradient descent methods to optimize the approximation of the bath correlation function. The coefficients g_j are real. However the frequencies ω_j are split into real and imaginary parts,

$$\omega_j = \alpha_j + i\gamma_j.$$

This ensures that the variational fitting process can optimize the parameters adequately and the program doesn't run into issues such as the difference between the bath correlation function and its approximation gradually increasing throughout the variational fitting process.

4 Methodology

4.1 Gradient Descent for Optimization

Gradient descent is mainly used for machine learning and optimization problems. Gradient descent seeks to find a local minimum of the cost function by adjusting model parameters [9]. In this work, we will utilize the gradient descent algorithm to optimize the parameters g_j and ω_j by minimizing the error between the original and approximated correlation function abiding the guidelines of the article "Create a Gradient Descent Algorithm with Regularization from Scratch in Python" by Turner Luke, see Ref.[9]. For our model optimization, we'll perform least squares optimization, where we seek to minimize the sum of the differences between our predicted values, and the data values[9]. The quadratic cost function is defined as:

$$C = \frac{\sum_{i=1}^{n}(y_i - \hat{y}_i)^2}{n} \tag{11}$$

where $\hat{y}_i$ is the model prediction from the independent variable. The model prediction is presented as a polynomial model.

$$\hat{y}_i = \beta_0 + \beta_1 x_i + ... + \beta_m x_i^m \tag{12}$$

As the name suggests, gradient descent algorithm optimizes the parameters to minimize the cost function by calculating the gradient of the cost, dependent on the independent variables. The gradient of the cost function is presented with the ∇ operator as

$$\nabla C = \frac{\delta C}{\delta \beta_0} + \frac{\delta C}{\delta \beta_1} + ... + \frac{\delta C}{\delta \beta_m}. \tag{13}$$

Fitting the parameters in such a way that descends the gradient enables a lesser cost, which is the objective of the minimization process. Updating the parameters g_j and ω_j, see 10, with their gradients allows the program to move in the direction of the steepest descent of the cost function. The gradient of the parameter are calculated and multiplied with the learning rate. This term is then subtracted from the parameter and the result of the subtraction is set as the updated parameter, respectively. The gradient contributions are then divided by the amount of timestamps, essentially averaging over time. This process is equivalent to computing the gradient of the mean squared error, which is normalized. The parameters are updated with a negative step along the gradient. This method exhibits a cost function, that iteratively decreases in value.

4.2 Numerical Implementation

4.2.1 Parameters

A Python implementation was developed using SciPy and NumPy to solve the optimization problem using the gradient descent algorithm. After the spectral density function and the bath correlation function are defined, see Eq.2 and 9, the typical range of the parameters that are not to be fitted is given, see Table 1. Starting off with the coupling strength η, this parameter represents the system-bath coupling strength The typical range of the values lie between 0.01 and 2, where $\eta \ll 1$ indicates weak coupling and shows a perturbative regime. Hence Markovian approximation is valid. On the other hand the range $\eta > 1$ indicates strong coupling and that the non-Markovian effects become significant [16][17]. The cutoff frequency ω_c determines the characteristic frequency scale of the bath. The value typically ranges from $0.01eV/\hbar$ to 10 $eV/\hbar$. A large value, e.g. $\omega_c \gg 1$, corresponds to a fast-decaying bath correlation function in terms of short memory effects and Markovian behavior. A small value however leads to a bath with long memory and strong non-Markovian effects [2][18].The choice of ω_c depends on the environment, where it should be large enough to capture all relevant bath modes but small enough to maintain numerical efficiency. Another parameter used is the inverse temperature β, where $\beta = 1/k_B T$. In natural units ($\hbar = k_B = 1$), the value range of the inverse temperature is typically described as $0.1\frac{1}{eV} \leq \beta \leq 10\frac{1}{eV}$. A high temperature regime corresponds to a small value of β (e.g. $\beta \ll 1$) and indicates the domination of thermal fluctuations. A low temperature regime on the other hand (e.g. $\beta > 5$) underlines the importance of the quantum effects [4]. The reduced Planck's constant $\hbar$ is often set to 1 in natural units. In terms of simplicity, this work will also set $\hbar$ to $1eVs$ [21]. The spectral density exponent s defines the type of the spectral density, see page 8. The typical values for s range from 0.5 to 2.

A random value among the typical range is assigned to each of these parameters every time the Python code is initialized. This results in varying values for the cost function but prevents the algorithm from over-fitting or adapting to constant parameters.

Parameter	Typical Range	Unit
Coupling Strength (η)	$0.01 \leq \eta \leq 2$	dimensionless
Cutoff Frequency ω_c	$0.01 \leq \omega_c \leq 10$	Hz (or energy: $J/\hbar, eV/\hbar$)
Inverse Temperature (β)	$0.1 \leq \beta \leq 10$	$1/eV$ (or s/J)
Reduced Planck's Constant ($\hbar$)	$\hbar \approx 1.054571817 \times 10^{-34}$	eVs (or Js)
Spectral Density Exponent (s)	$0.5 \leq s \leq 2$	dimensionless

Table 1: Parameters, The Typical Range of Their Values and the Units

4.2.2 Approximation and Optimization

Using the randomly initialized parameters, a set of discrete values for $C(t)$ are generated using the definition in Eq.9. The discrete values are to be used to fit the sum of exponential functions C_{approx}, see Eq.10, to the original bath correlation function. The Python code behind the variational fitting process can be simply presented as:

Algorithm 1 Variational Fitting of the Bath Correlation Function as a Sum of Exponential Functions

$t_{vals} \leftarrow$ time values
$J(\omega) \leftarrow \eta\omega^s e^{-\frac{\omega}{\omega_c}}$
$C(t) \leftarrow \frac{1}{2\pi}\int_{-\infty}^{\infty} J(\omega)\left[coth\left(\frac{\beta\hbar\omega}{2}\right)+1\right]e^{-i\omega t}d\omega$
$C_{vals}(t) \leftarrow$ discrete values of $C(t)$
$C_{approx}(t) \leftarrow \sum_{j=1}^{K} g_j e^{-i\omega_j t}$
error $\leftarrow C_{approx}(t) - C_{vals}(t)$
cost $\leftarrow \sum_t |C_{vals}(t) - C_{approx_{vals}}(t)|^2 + \lambda_{reg}(\sum_j g_j^2 + \sum_j |\omega_j|^2)$
if t in t_{vals} **then**
    Compute C_{approx}
    Compute error
else if j in K **then**
    for each j in K
    Compute expterm $= e^{-i\omega_j t}$
    if the number of iterations is 0 **then**
        for each iteration to a selected number of max. iterations
        Compute the gradients $grad_j, grad_{\omega r}, grad_{\omega i}$ utilizing **L2 regularization** 4.2.3
        Update Parameters g_j and ω_j using the learning rate and the gradients
        Return updated g_j,ω_j
        Set previous cost to ∞
        Compute cost function with updated g_j, ω_j
        if |previous cost - cost| is less than the given threshold **then**
            Set previous cost = cost
            Print the cost every 10th iteration
            Return optimized g_j, ω_j
        end ifthe optimized parameters are presented
    end ifthe number of iteration reaches max. iterations
    Plot results with the optimized parameters
end ifthe optimization process is complete and the results are plotted.

4.2.3 L2 Regularization

The L2 regularization, also known as the Ridge regression, is a method used to produce stable estimates of the coefficients [22]. The Ridge regression is often used to alleviate the overfitting in machine learning models. Overfitting can occur in different ways. With our optimization problem, the coefficients g_j and ω_j becoming too large can cause overfitting, forcing the approximation to follow the exact details of the given data or the noise rather than the true function. Another cause of overfitting can be the use of too many exponential terms K, see 10, in the summation. In that case, the approximation might fit the training data perfectly but fail to generalize to new time values. To mitigate overfitting, L2 regularization introduces a penalty term to the cost function to keep them from becoming too extreme 3. The penalty term

$$\lambda_{reg}(\sum_j g_j^2 + \sum_j |\omega_j|^2) \tag{14}$$

is then added to the cost function. Hence, the value of the cost function also increases with extreme parameter values, and the cost minimization algorithm prioritizes the parameters with less extreme values.

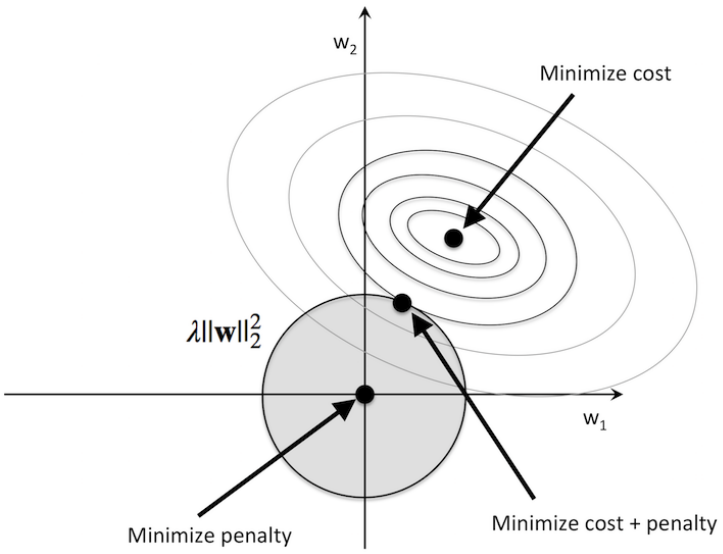

Figure 3: L2 Regularization

4.2.4 K Regularization

K regularization is not a formal mathematical method, but an implicit implementation we evaluated in our Python code. K regularization simply consists of scaling the learning rate with the number of exponential terms K. With higher K, the process exhibits higher computational complexity. By scaling the learning rate proportional to $1/\sqrt{K}$, we enable a lower learning rate for higher K, therefore, more stability. K regularization is another method that one may use if overfitting occurs despite L2 regularization. In itself K regularization doesn't enable greater stability than L2 regularization, see Fig. 9. In the prospects of our work, L2 regularization is sufficient. One may choose to use K regularization as a supplementary form of stability. K regularization fundamentally controls model complexity.

5 Results and Discussion

In this section, we evaluate the accuracy of the variational fitting method used to approximate the bath correlation function $C(t)$. The initial fitting curves in Fig. 4 and Fig. 5 are generated using parameters that are randomly assigned from a range of their typical values. The initialization plotted by these figures consists of a total of 100 time-discrete values of the bath correlation function in a span of 5 seconds. As expected, the approximation in this stage is poor, as the randomly chosen parameters do not effectively capture the structure of the bath correlation function. This results in significant deviations between $C_{original}(t)$ and $C_{approx}(t)$, see Figures 45.

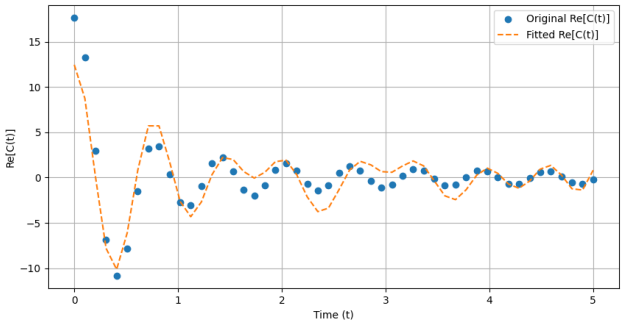

Figure 4: Initial Fit for the Real Part of $C(t)$

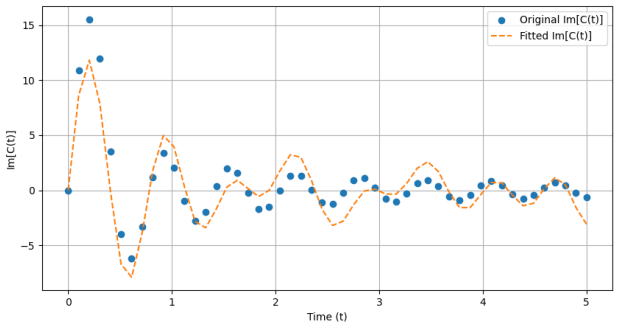

Figure 5: Initial Fit for the Imaginary Part of $C(t)$

The parameters from the initial fit are then regulated and updated with their gradients. Hereby, the parameter ω_j, see equation 10, is separated into a real part α_j and an imaginary part γ_j. The gradients of both parts are calculated and the fitted to the initial parameter to prevent additional error due to ω_j being complex. Figure 6 shows the original and the approximated bath correlation functions calculated with the parameters optimized with gradient descent and L2 regularization. The approximation struggles at small time values, then improves over time. This is largely because of the relation of the exponential terms and $C_{approx}(t)$ at $t = 0$. At $t = 0$, all exponential terms are equal to 1, so the approximated bath correlation function solely depends on the sum of coefficients g_j. But the original $C(t)$ at $t = 0$ depends on an integral over the full spectral density, hence it exhibits a much richer structure. This results in a better fit at later times, where exponential terms start to differentiate themselves. Despite the visible deviation near $t = 0$ in both real and imaginary parts, the fit is satisfactory overall, especially after $t > 1$. The oscillatory behavior is captured in phase and amplitude. This model succeeds to capture the dominant dynamics of the correlation function. The early-time error is expected, due to all exponential terms evaluating to 1, making it difficult to model steep features or derivative discontinuities. The inaccuracy is addressed by emphasizing early-time behavior using weighted time values, where the sampling near $t = 0$ have more impact in regards to later time values. This solution however yields a similar result, since the deviation is expected because of the limited control over sharp initial features.

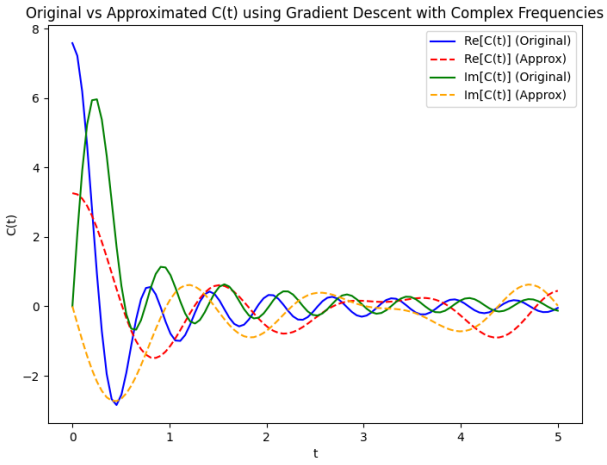

Figure 6: Original vs Approximated $C(t)$ Using the Parameters Optimized with Gradient Descent and L2 Regularization

As seen in Figure 5, gradient descent reduces the costs efficiently with each iteration. Whereas within approximately 100 iterations, the value of the cost function is negligible. The higher initial cost values stem from the initial fit, where the initially fitted function greatly deviates from the original correlation function. The cost consists of the absolute difference between the original and the approximated correlation function, and also the regularization term, understandably, see section 4.2.2. It is observable, that the gradient descent algorithm minimizes the cost efficiently, as intended.

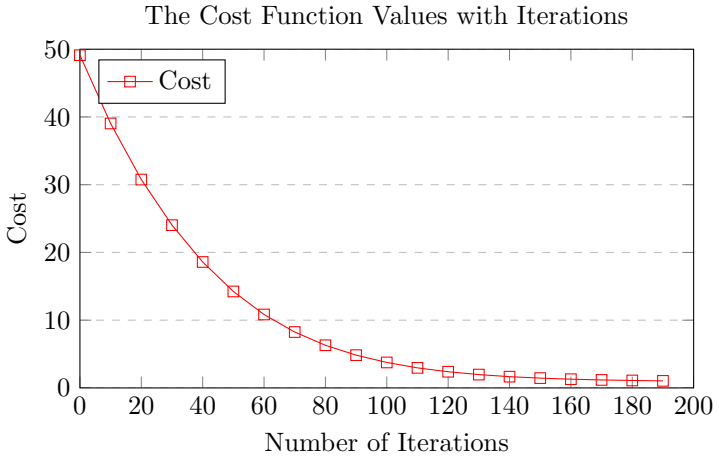

Figure 7: The Cost Function Values with Iterations, Increments of 10

Figure 8 exhibits the absolute approximation error $|C_{vals}(t) - C_{approx_{vals}}(t)|$ as a function of time for varying values of the number of exponential terms K in $(5, 10, 20, 30, 50)$, see 10. As K increases the approximation error consistently decreases, especially for intermediate to long times ($t > 1$). Low values for K indicate a lower amount of exponential terms, which are to be summed to express the original correlation function. Hence, for lower values the the approximation is limited in flexibility to capture the full structure of $C(t)$, leading to higher persistent error. Even for high K, the error at $t = 0$ remains non-negligible, further emphasizing the challenge in matching the sharp features of the original function at early times. This behavior illustrates the typical trade-off between model complexity and approximation accuracy. A larger K introduces more parameters and increases the expressive power of the exponential sum, allowing for better fitting. However, without proper regularization, higher K can also increase the risk of overfitting or numerical instability. In regards of model complexity and algorithm runtime, we found $K = 30$ to be a suitable value for this work, enabling decent runtime.

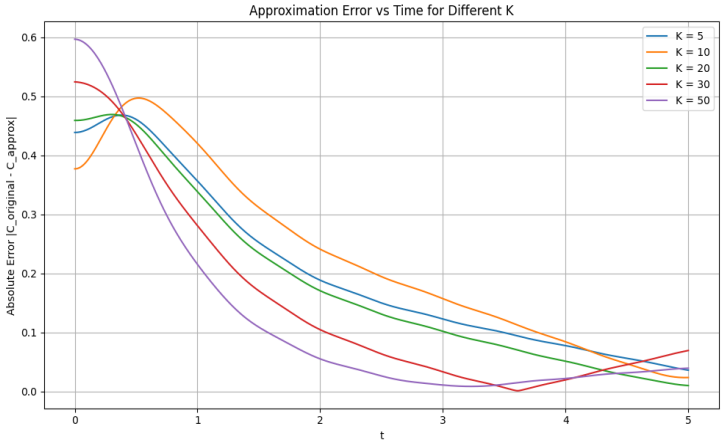

Figure 8: Approximation Error Plotted by Time for Different Values of K

To further analyze model performance, we evaluated three regularization strategies using a fixed set of parameters. The strategies in question are no regularization, L2 regularization and K regularization. Figure 9 displays the absolute error over time for each case. It is visible that L2 regularization yields the lowest and smoothest error, especially after the initial transient region. Although it might seem as no regularization is performing as well as L2 regularization, the no regularization strategy is unpredictable and unstable. No regularization is heavily dependent on the initialization of the parameters, making it more susceptible to overfitting. If overfitting occurs, which is observable more often with no regularization in comparison to the other strategies, there is not a curve for no regularization to be observed. The program fails to fit the approximation to the original function. K regularization on the other hand exhibits large oscillations and peaks in the error, indicating poor convergence or underfitting. Hence, supporting the initial argument, that K regularization is to be used as a supplementary form of regularization in addition to L2 regularization. L2 regularization is crucial to the stabilization of the optimization process. It enables the suppression of large parameter magnitudes, encourages smoother fits, and avoids overfitting. The learning rate scaling (K-Regularization), while theoretically valid, under-performs in practice due to overly conservative updates, leading to poor convergence. Thus, L2 regularization is clearly the more robust and effective regularization method in this setting. These results confirm that both the choice of K and the regularization method significantly affect the approximation performance. L2 regularization with a moderately large K ($e.g., 30, 50$, or higher) yields the best trade-off between accuracy and stability.

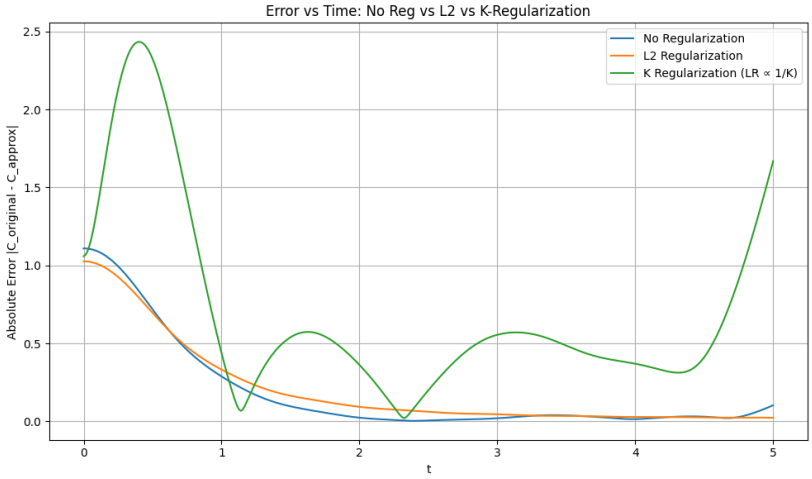

Figure 9: Error Plotted by Time for No Regularization, L2 Regularization and K Regularization

Strategy	Error Near $t = 0$	Long-Time Accuracy	Stability
Small K	High error	Poor	Stable
Large K	Slightly better	Very good	Can be unstable without regularization
L2 Regularization	Moderate	Best	Very stable
K Regularization	Very high error	Poor	Unstable

Table 2: Evaluation of Regularization Strategies

6 Conclusion

This thesis presents a variational fitting approach for the bath correlation function using a sum of exponential functions. This approach is motivated by the need to efficiently and accurately represent open quantum system dynamics, where the bath plays a critical role in introducing memory effects and dissipation. The core of the method involved formulating $C(t)$ as a sum of exponential functions, see 10, where g_j are real coefficients and ω_j are complex frequencies to be optimized using gradient descent. To evaluate the performance of the approximation, we analyzed the convergence behavior and accuracy of the method under different values of K and different regularization strategies. Our findings overall include that the approximation tends to perform best at intermediate to long times, while errors at early times remain a challenge due to structural limitations of the exponential representation. The accuracy of the approximation could be further amplified by implementing even higher values of K and higher numbers of maximum iterations for the gradient descent algorithm. With regards to computational effort and runtime, this work was conducted with an interval of $(5 - 50)$ for K and $(100 - 1000)$ maximum iterations for gradient descent. L2 regularization in addition to the selection of a large K value proves to be the best strategy in terms of long-time accuracy and stability. This work demonstrates that a variational exponential sum is a viable and flexible tool for modeling bath correlation functions, particularly when combined with proper regularization. It opens the door to further improvements, including adaptive basis selection, frequency-domain fitting, integration with non-Markovian quantum dynamic solvers and the introduction of machine learning techniques to enhance optimization. Future research directions could include reevaluation using Debye spectral density, exploring different functional bases beyond exponential functions (e.g., Gaussian or Lorentzian functions), and extending the method to multidimensional correlation functions in more complex quantum environments.

Overall, this study provides a practical and adaptable framework for spectral decomposition in open quantum systems, contributing to more accurate simulations in quantum chemistry, condensed matter, and quantum technologies.

7 List of Figures

List of Figures

1 Schematics of the total system consisting of the two-state system TSS and the bath B 7
2 $J(\omega)/(\eta\omega_c)$ plotted in terms of ω/ω_c 9
3 L2 Regularization 14
4 Initial Fit for the Real Part of $C(t)$ 16
5 Initial Fit for the Imaginary Part of $C(t)$ 16
6 Original vs Approximated $C(t)$ Using the Parameters Optimized with Gradient Descent and L2 Regularization 17
7 The Cost Function Values with Iterations, Increments of 10 . . . 18
8 Approximation Error Plotted by Time for Different Values of K . 19
9 Error Plotted by Time for No Regularization, L2 Regularization and K Regularization 20

List of Tables

1 Parameters, The Typical Range of Their Values and the Units . 12
2 Evaluation of Regularization Strategies 20

8 Bibliography

References

[1] G. Ritschel and A. Eisfeld; *Analytic Representations of Bath Correlation Functions for Ohmic and Superohmic Spectral Densities Using Simple Poles*; In: Journal of Chemical Physics (2014), doi: 10.1063/1.4893931 .

[2] U.Weiss; *Quantum Dissipative Systems*; World Scientific Publishing Company; 3 edition (2012),doi: 10.1142/4239 .

[3] V. May and O. Kühn; *Charge and Energy Transfer Dynamics in Molecular Systems*; WILEY-VCH (2000), doi: 10.1002/9783527633791 .

[4] H.-P. Breuer and F. Petruccione; *The Theory of Open Quantum Systems*; Oxford University Press (2002), doi: 10.1093/acprof:oso/9780199213900.001.0001 .

[5] S. Valleau, A. Eisfeld, and A. Aspuru-Guzik; *On the Alternatives for Bath Correlators and Spectral Densities from Mixed Quantum-classical Simulations*; In: Journal of Chemical Physics (2012), doi: 10.1063/1.4769079 .

[6] M. Grifoni, E. Paladino, and U. Weiss; *Dissipation, decoherence and preparation effects in the spin-boson system.* In: The European Physical Journal B-Condensed Matter and Complex Systems 10 (1999), doi: 10.1007/s100510050903 .

[7] D. W. Schönleber, A. Croy, and A. Eisfeld; *Pseudomodes and the corresponding transformation of the temperature-dependent bath correlation function.*; In: Physical Review A 91 (2015), doi: 10.1103/PhysRevA.91.052108 .

[8] J. B. Gilmore and R. H. McKenzie; *Criteria for quantum coherent transfer of excitations between chromophores in a polar solvent.* In: Chemical Physics Letters 421. 1-3(2006), doi: 10.1016/j.cplett.2005.12.104 .

[9] T. Luke; *Create a Gradient Descent Algorithm with Regularization from Scratch in Python*; https://towardsdatascience.com/create-a-gradient-descent-algorithm-with-regularization-from-scratch-in-python-571cb1b46642/;(2022).

[10] T. A. Costi and R. H. McKenzie; *Entanglement between a qubit and the environment in the spin-boson model.* ; Physical Review A 68.3; (2003), doi: 10.1103/PhysRevA.68.034301 .

[11] Y. Yan, R. Xu, Y. Mo, and P. Cui; *Non-Markovian Quantum Dissipation in the Presence of External Fields*;(2003), doi: 10.1007/978-94-017-0635-3_2 .

[12] J. Barr, G. Zicari, A. Ferraro, and M. Paternostro; *Spectral Density Classification For Environment Spectroscopy*; (2024), doi: 10.1088/2632-2153/ad2cf1 .

[13] S. A. Egorov, K. F. Everitt, and J. L. Skinner; *Quantum Dynamics and Vibrational Relaxation*; (1999), doi: 10.1021/jp9919314 .

[14] B. J. Berne and G. D. Harp; *On the calculation of time correlation functions*; in Advances in Chemical Physics (Wiley, 1970); pp. 63–227, doi: 10.1002/9780470143636.ch3 .

[15] Y. Yan and R. Xu; *Quantum Mechanics of Dissipative Systems*; Ann. Rev. Phys. Chem. 56; 187 (2005), doi: 10.1146/annurev.physchem.55.091602.094425 .

[16] M. B. Plenio and P. L. Knight; *The quantum-jump approach to dissipative dynamics in quantum optics*; Rev. Mod. Phys. 70, 101; (1998), doi: 10.1103/RevModPhys.70.101 .

[17] A. Nazir and G. Schaller; *The Reaction Coordinate Mapping in Quantum Thermodynamics*; in Thermodynamics in the Quantum Regime; Springer; (2019), doi: 10.48550/arXiv.1805.08307 .

[18] A. J. Leggett, S. Chakravarty, A. T. Dorsey, M. P. A. Fisher, A. Garg, and W. Zwerger; *Dynamics of the dissipative two-state system*; Rev. Mod. Phys. 59, 1; (1987), doi: 10.1103/RevModPhys.59.1 .

[19] R. Egger, C. H. Mak, and U. Weiss; *Quantum dynamics of a dissipative two-state system*; Phys. Rev. E 50, 6; (1994), doi: 10.1103/PhysRevB.43.5397 .

[20] M. Thorwart, P. Reimann, P. Jung, and R. Fox; *Quantum damped harmonic oscillator: Exact simulation of time-dependent relaxation*; Chem. Phys. 235, 1-3; (1998), doi: 10.3938/jkps.67.404 .

[21] J. J. Sakurai and J. Napolitano; *Modern Quantum Mechanics*; Addison-Wesley; (2011), .

[22] D. E. Hilt and D. W. Seegrist; *Ridge, a computer program for calculating ridge regression estimates*; Upper Darby, Pa, Dept. of Agriculture, Forest Service, Northeastern Forest Experiment Station; (1977), doi: 10.5962/bhl.title.68934 .